Sulfated Zirconia Catalysts. The Crystal Phases and Their Transformations

Ram Srinivasan,[†] Thomas R. Watkins,[‡] Camden R. Hubbard,[‡] and Burtron H. Davis*,[†]

Center for Applied Energy Research, University of Kentucky, 3572 Iron Works Pike, Lexington, Kentucky 40511, and High Temperature Materials Laboratory, Oak Ridge National Laboratory, Oak Ridge, Tennessee 37831

Received November 7, 1994. Revised Manuscript Received January 9, 1995[⊗]

The phase transformations of zirconia are an important factor that makes it a valuable material for numerous applications in ceramics. The factors triggering the onset of the phase transformation are controversial. Evidence is presented to show that surface sites that adsorb oxygen at low temperatures (298–500 K) are responsible for causing the tetragonal → monoclinic transformation at low temperatures. The incorporation of sulfate covers these sites and inhibits the tetragonal → monoclinic transformation.

Introduction

Zirconia is used in a number of applications, such as making tough ceramics, engine parts, solid electrolytes, etc. It can also be used as a catalytic material or support with unique properties. Zirconia exists in several crystalline forms: monoclinic, tetragonal, cubic, and orthorhombic. Although the monoclinic phase is stable below about 1150 °C, the tetragonal phase may, under certain conditions, be present as a metastable phase at lower temperatures. Several explanations for the low-temperature stabilization of the tetragonal phase have been advanced. However, the mechanism of stabilization of tetragonal ZrO_2 at low temperatures is not fully understood.

The metastable tetragonal-phase stability has been attributed to the lower surface energy for the tetragonal phase than for the monoclinic phase.[1-3] It was estimated, based on surface energy effects, that the critical size for the stabilization of the tetragonal phase was about 30 nm.[2] Thus, crystallites smaller than 30 nm could exist in the tetragonal form, but particles larger than this size would tend to transform to the more stable monoclinic form. Small amounts (about 0.75 wt %) of bound OH groups in the solid solution were suggested to stabilize the tetragonal form at room temperature; thus, when the solid was heated in the region 600–900 °C, the OH groups were driven off as water vapor and the formation of monoclinic phase was observed.[4] However, Clearfield[5] showed that the sequence of phase transformation in hydrous ZrO_2 precipitate was

[amorphous] → [tetragonal + monoclinic] → [monoclinic]

The presence of water vapor was observed to increase surface diffusion and thus enhance crystallite growth because of the decrease in the surface energy which stabilized the tetragonal phase.[6,7] The large amount of water present during calcination was proposed to catalyze the $t \rightarrow m$ transformation in zirconia.

Morgan[8] showed that ultrafine monoclinic zirconia particles of 6 nm in size could be produced after extensive refluxing of zirconyl chloride at a pH of 1–2. Morgan[8] therefore questioned whether surface energy factors inhibiting the $t \rightarrow m$ transformation and cautioned that a strict conclusion as to the relative stabilities was almost impossible.

X-ray and neutron diffraction studies on amorphous ZrO_2 have shown that certain preferred interatomic spacings exist and the atoms in amorphous zirconia are not distributed at random.[9] These interatomic spacings, characteristic of short-range order, correspond to the distances observed in tetragonal ZrO_2. In other words, the interatomic Zr–Zr and Zr–O distances in amorphous precursor gel were similar to the corresponding ones in the tetragonal structure. Thus, amorphous ZrO_2 contains tetragonal ZrO_2 nuclei, which can grow during crystallization under hydrothermal conditions. Therefore, the metastability of the tetragonal ZrO_2 was attributed to the structural similarities between a precursor amorphous phase and the tetragonal phase.[9] A mechanism of topotactic crystallization of t-ZrO_2 on nuclei in the amorphous ZrO_2 was proposed for the $t \rightarrow m$ transformation.[10]

It has been proposed that the domain boundaries inhibited the $t \rightarrow m$ transformation, and when an active nucleation site was available, the transformation would occur at low temperatures.[11] The low-temperature $t \rightarrow m$ transformation in ZrO_2 was termed to be martensitic similar to the high-temperature $t \rightarrow m$ transformation and repudiated the view of tetragonal-phase stabilization based on surface energy theory. Another view is that initial nucleation of t-ZrO_2 is favored by anionic

[†] University of Kentucky.
[‡] Oak Ridge National Laboratory.
[⊗] Abstract published in *Advance ACS Abstracts,* February 15, 1995.

(1) Garvie, R. C. *J. Phys. Chem.* **1965**, *69*, 1238.
(2) Garvie, R. C. *J. Phys. Chem.* **1985**, *82*, 218.
(3) Garvie, R. C.; Swain, M. V. *J. Mater. Sci.* **1985**, *20*, 1193.
(4) Cyprês, R.; Wollast, R.; Raucq, J. *Ber. Dtsch. Keram. Ges.* **1963**, *40*, 527.
(5) Clearfield, A. *Inorg. Chem.* **1964**, *3*, 146.
(6) Murase, Y.; Kato, E. *J. Am. Ceram. Soc.* **1983**, *66*, 196.
(7) Murase, Y.; Kato, E. *J. Am. Ceram. Soc.* **1979**, *62*, 527.
(8) Morgan, P. E. D. *J. Am. Ceram. Soc.* **1984**, *67*, C-204.
(9) Livage, J.; Doi, K.; Mazieres, C. *J. Am. Ceram. Soc.* **1968**, *51*, 349.
(10) Tani, E.; Yoshimura, M.; Somiya, S. *J. Am. Ceram. Soc.* **1983**, *66*, 11.
(11) Mitsuhashi, T.; Ichihara, M.; Tatsuke, U. *J. Am. Ceram. Soc.* **1974**, *57*, 97.

0897-4756/95/2807-0725$09.00/0

vacancies with trapped electrons, and only at high temperatures when the electronic defects disappear, the crystallites grow so that the monoclinic phase nucleates.[12]

Data obtained using in situ high-temperature X-ray diffraction indicated that the $t \rightarrow m$ transformation initiating site was predominantly an oxygen-deficient surface site.[13,14] In this investigation, further evidence, using TGA/DTA data combined with the high-temperature X-ray diffraction data, is presented to show that the oxygen deficient surface sites are the source for initiating the $t \rightarrow m$ transformation in zirconia at low temperatures.

Experimental Methods

Preparation of Catalysts. Zirconium oxide was prepared by rapidly precipitating from a 0.3 M solution prepared from anhydrous $ZrCl_4$ with an excess amount of NH_4OH at a pH of 10.5. After washing the precipitate thoroughly with water and then with ethanol, it was dried at 120 °C overnight. The chloride content of the last wash filtrate was <3 ppm. The dried, hydrous zirconia powders were sulfated using 15 mL of 0.5 M H_2SO_4/g of catalyst. The slurry containing ZrO_2 powders and the appropriate quantity of H_2SO_4 was stirred for 2 h; then the solid was collected, without further washing, and dried at 120 °C overnight. The chemical analysis showed that this sample, designated as SO_4^{2-}/ZrO_2, contained about 3.46 wt % S; i.e., 10.4 wt % SO_4^{2-}. A portion of this sulfated ZrO_2 was impregnated with a hexachloroplatinate solution using the *incipient wetness* technique to obtain a Pt loading of 0.6 wt %. After platinum impregnation, the sample was dried at 120 °C overnight; chemical analysis showed the presence of 0.57 wt % Pt. This sample will be designated as $Pt-SO_4^{2-}/ZrO_2$.

About 20 g of the freshly prepared $Pt-SO_4^{2-}/ZrO_2$ sample was reduced in flowing hydrogen in a quartz tubular reactor at 725 °C for 2 h and cooled to room temperature rapidly. This sample was exposed to air after reduction and sulfur analysis showed that this sample contained only about 0.15 wt % S.

X-ray Diffraction (Room Temperature). Room-temperature X-ray diffraction was carried out using a Rigaku X-ray diffractometer at 40 kV, 20 mA, which was equipped with a graphite monochromator on the diffracted beam path. All scans were done with a 0.02° step, but certain 2θ regions of importance were scanned with a 0.01° step. The scan time was 5 s/step. For room-temperature XRD, the samples were calcined in a muffle furnace in air at the desired temperature prior to the XRD analysis.

X-ray Diffraction (High Temperature). High-temperature X-ray diffraction studies were carried out using a Scintag PAD V X-ray diffractometer, equipped with a $\theta-\theta$ goniometer, and a position-sensitive detector. This diffractometer has been described elsewhere.[14] The hydrogen treatment studies were conducted using the in situ high-temperature X-ray diffraction technique. A few milligrams of $Pt/SO_4^{2-}/ZrO_2$ powders were mixed with absolute alcohol, and two or three drops was placed on a silica plate placed on a platinum heating strip. After evacuation of the X-ray chamber, H_2 was introduced at a flow rate of 50 mL/min. The sample was heated at a rate of 20 °C/min to 500 °C, and an XRD pattern was collected at 500 °C. Then the sample was heated to 550 °C, and another XRD pattern was taken at this temperature. Likewise, XRD patterns were collected at 600 and 725 °C. The sample was then rapidly cooled to room temperature by turning off the power to the furnace. An XRD pattern was collected at room temperature in flowing H_2. Then the furnace was opened and the sample was exposed to air, and after exposure to air a room-temperature XRD pattern was collected from this air-exposed sample.

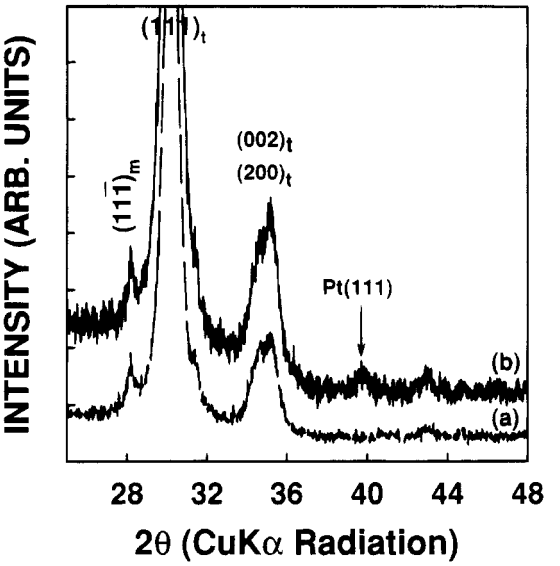

Figure 1. X-ray diffraction patterns obtained from the samples after activation at 725 °C in air for 2 h: (a) $SO_4^{2-}-ZrO_2$ and (b) $Pt-SO_4^{2-}-ZrO_2$.

Transmission Electron Microscopy (TEM). The transmission electron microscopy (TEM) technique was used to obtain complementary evidence for particle size and morphology. A Hitachi H800NA scanning electron microscope was used at 200 kV. For microdiffraction, a 5 nm electron probe was used.

High-Resolution Electron Microscopy (HREM). A small portion (about 4–6 mg) of the catalyst was suspended in absolute ethanol, and this suspension was agitated in an ultrasonic bath. A drop of the suspension was placed on a carbon-coated 200 mesh copper grid. This grid was introduced into the microscope. High-resolution electron microscopy studies were conducted using a JEOL 4000EX outfitted with a vertical-entry six-specimen holder. The operating voltage was 400 kV and the lattice resolution of the microscope was 0.15 nm.

Results and Discussion

The X-ray diffraction patterns of the $SO_4^{2-}-ZrO_2$ and $Pt-SO_4^{2-}-ZrO_2$ catalysts after activation in air at 725 °C for 2 h are presented in Figure 1. The activation at 725 °C was adopted since this produced the most active catalyst for hexadecane conversion.[15] The X-ray diffraction patterns (Figure 1) indicate that both samples have the tetragonal form.

The region of $2\theta = 36-48°$ for the $Pt-SO_4^{2-}-ZrO_2$ sample (Figure 2) clearly shows the presence of metallic platinum, since both Pt (111) and Pt (200) profiles are present. Thus, metallic platinum was observed after the sample was calcined in air at 725 °C for 2 h. This result was corroborated by high-resolution electron microscopy and agrees with other reports.[16,17] In Figure 3, several lattice fringes for metallic platinum and for tetragonal ZrO_2 are observed for the $Pt-SO_4^{2-}-ZrO_2$ sample. A transmission electron micrograph from this catalyst is presented in Figure 4, and an electron microdiffraction pattern from a Pt particle is also shown in the inset of Figure 4. The Pt particle size obtained

(12) Osendi, M. I.; Moya, J. S.; Serna, C. J.; Soria, J. *J. Am. Ceram. Soc.* **1985**, *68*, 135.
(13) Srinivasan, R.; Davis, B. H.; Cavin, O. B.; Hubbard, C. R. *J. Am. Ceram. Soc.* **1992**, *75*, 1217.
(14) Srinivasan, R.; Cavin, O. B.; Hubbard, C. R.; Davis, B. H. *Chem. Mater.* **1993**, *5*, 27.
(15) Srinivasan, R.; Keogh, R. A.; Davis, B. H., submitted.
(16) Zhao, J.; Huffman, G. P.; Davis, B. H. *Catal. Lett.* **1994**, *24*, 385.
(17) Sayari, A.; Dicko, A. *J. Catal.* **1994**, *145*, 561.

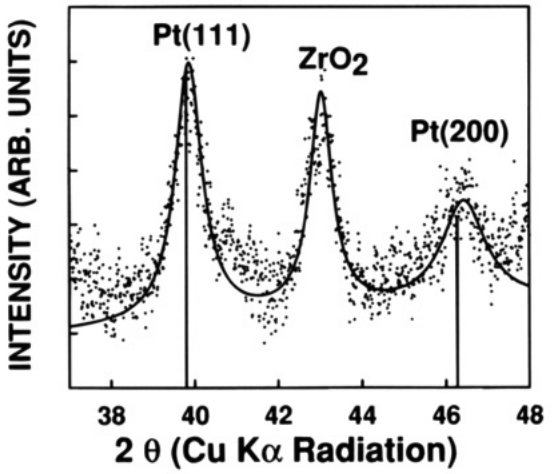

Figure 2. X-ray diffraction pattern in the 2θ range of 37–48° obtained from the Pt–SO_4^{2-}–ZrO_2 sample after activation at 725 °C in air for 2 h. The raw data are represented as scattered points, and a Lorentzian is fit to the data.

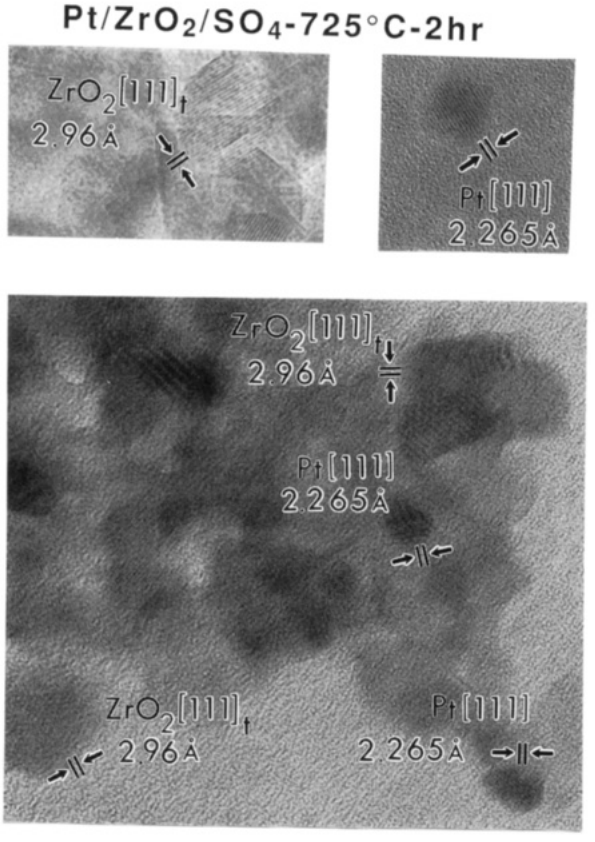

Figure 3. High-resolution electron micrographs obtained from the sample Pt–SO_4^{2-}–ZrO_2, showing Pt (111) and (200) lattice fringes as well as tetragonal ZrO_2 lattice fringes.

from transmission electron microscopy, ranges from 4 to 6 nm, and agrees with the value of 6 nm calculated from the XRD line width at half maximum intensity using the Debye-Scherrer equation.[18] Thus, the presence of metallic platinum following activation in air at 725 °C is well documented. The reduction of platinum species to metallic platinum occurs after activation in air at 725 °C but not at the lower temperatures used in this study. Several samples calcined at 400, 500, and 600 °C in air did not exhibit the presence of metallic platinum and only showed XRD patterns for tetragonal ZrO_2. Some samples were calcined in air at 500 °C for times ranging from 2 to 67 h, and the formation of metallic platinum was not observed by XRD. Peaks for platinum oxide were not observed either.

The surface area of the dried hydrous zirconia prior to calcination was 230 m^2/g. Following calcination at 500 °C for 67 h, the surface area was 135 m^2/g; without the presence of sulfate the surface area was 75 m^2/g. It has been reported that the presence of sulfate stabilizes the tetragonal phase of zirconia and causes the retention of a high surface area after calcination (for example, ref 19).

The sample Pt–SO_4^{2-}–ZrO_2 was subjected to high-pressure reaction conditions. After activation in air at 725 °C for 2 h, the catalyst was immediately transferred into a batch reactor and the reactor was sealed with minimum exposure to air. The conversion of methylcyclohexane (MCH) was carried out at 150 °C at 500 psig for 15 min. After this reaction period, the catalyst was removed from the reactor and was subjected to characterization studies. The X-ray diffraction pattern obtained from this catalyst indicated the same phases as the sample activated at 725 °C for 2 h. The XRD data show the formation of metallic platinum in addition to the tetragonal phase of ZrO_2. Other phases, such as platinum oxide or sulfide, were not observed.

The XRD pattern obtained from the sample Pt–SO_4^{2-}–ZrO_2, following the TG/DTA/MS analysis in air was similar to the one shown in Figure 2; i.e., the formation of metallic platinum was observed for the sample treated in air in the TGA/DTA furnace following heating to 800 °C at 10 °C/min. The XRD pattern in Figure 5 and the 2θ region of 36–48°, plotted on an expanded scale (Figure 5b) from the sample following treatment in H_2 in the TGA/DTA show that the XRD peaks corresponding to the formation of metallic platinum were absent, and a partial transformation from the tetragonal to monoclinic phase of ZrO_2 occurred. Therefore, in situ high-temperature X-ray diffraction was carried out for this sample in a flow of H_2. The X-ray diffraction patterns recorded after heating at 500, 550, and at 725 °C are presented in Figure 6. The XRD peaks for the metallic platinum were not observed after heating to 725 °C in H_2, and only the tetragonal ZrO_2 was observed. The XRD pattern from this sample after it was rapidly cooled to room temperature in hydrogen showed only the peaks for major tetragonal phase and no metallic platinum peaks (Figure 7a). After exposure to air at room temperature, about 40% of the tetragonal phase was transformed to monoclinic phase (Figure 7b). This is consistent with the view that the phase transformation was caused by oxygen-deficient surface sites of ZrO_2.[13] The sulfur content of this sample was only 0.15 wt % after treatment in H_2, whereas it would be about 1 wt % if the sample had been heated in air to the same temperature. This suggests that in the flow of H_2, the sulfate ions react with H_2 to form H_2S and H_2O, and this was shown, by mass spectrometry studies, to be the case.[15] Thus, the hydrogen treatment at 725 °C removes a larger amount of sulfur from the sample than the treatment in air.

(18) Klug, P.; Alexander, L. E. *X-ray Diffraction Procedures*; Wiley: New York, 1967; p 491.

(19) Chokkaram, S.; Srinivasan, R.; Milburn, D. R.; Davis, B. H. *J. Colloid Interface Sci.* **1994**, *165*, 160.

(20) Srinivasan, R.; Taulbee, D.; Davis, B. H. *Catal. Lett.* **1991**, *9*, 1.

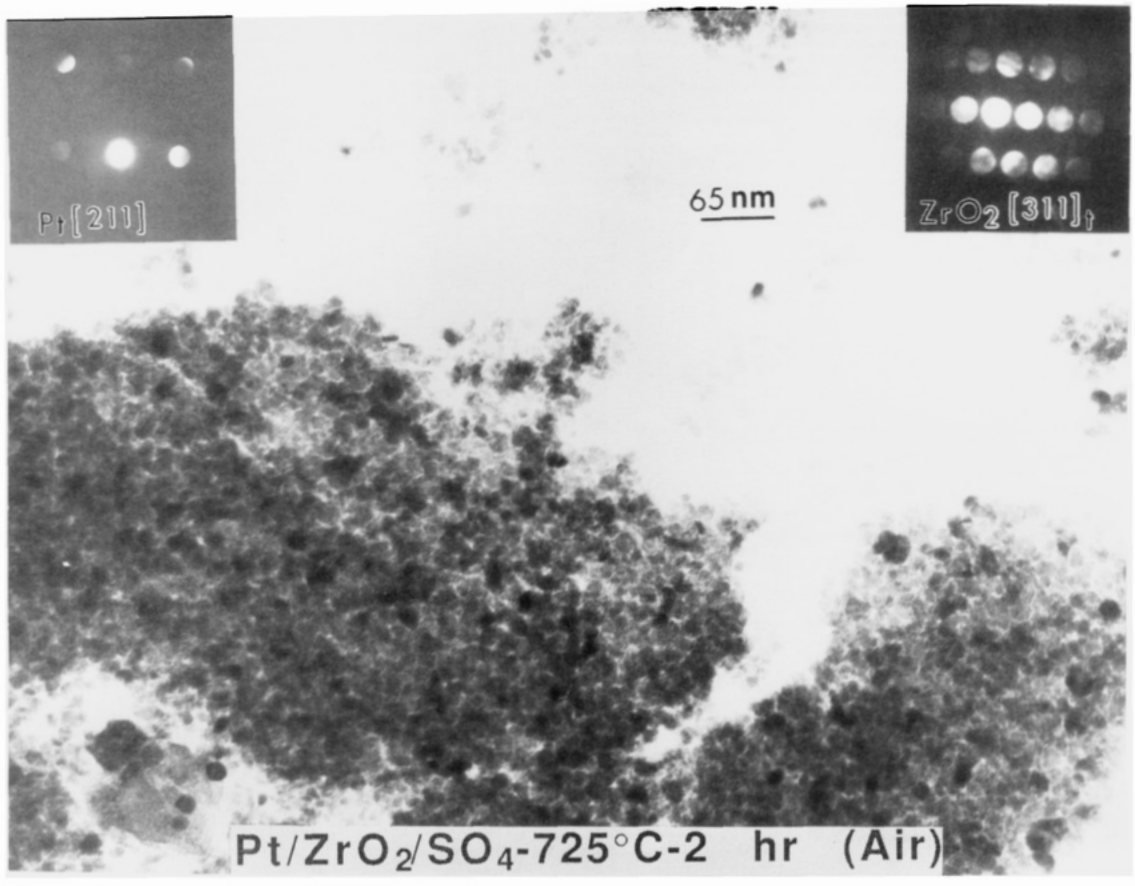

Figure 4. Transmission electron micrograph from the sample $Pt-SO_4^{2-}-ZrO_2$, and the electron microdiffraction pattern from a platinum particle.

Clearfield[21] offers an explanation for the dependence of the zirconia phase on the pH and/or rate of precipitation. He postulates that the zirconia surface is fully hydroxylated by OH^- bridges. On heating, these hydroxyls split out water yielding half as many oxygens on the surface and many open coordination sites on the Zr atoms. The heating reaction therefore causes a reaction with the stoichiometry shown in the following equation:

$$2(OH)^-_{br} \rightarrow O^{2-} + H_2O \qquad (1)$$

The hypothesis is made that the surface oxide ions that are formed by eq 1 then shift to cover the open coordination sites, triggering the $t \rightarrow m$ phase transformation. The reason for the different behavior is that the rapid precipitation leads to a polymer that is much less organized than the slowly precipitated material. Direct evidence to substantiate this model is, at best, very limited.

On the other hand, there are several experimental observations that are well founded and relate to the phase transformation. These include the following:

(1) For materials prepared by precipitation to produce a final pH of 10.4, both rapidly precipitated ($RP-ZrO_2$) and slowly precipitated ($SP-ZrO_2$) samples exhibit an exotherm at about 450 °C when heated at 20 °C/min in an inert or an air atmosphere, and the same amount of heat is liberated by the two samples.[22]

(2) $RP-ZrO_2$ and $SP-ZrO_2$ both transform during the exotherm from an X-ray amorphous material to a crystalline material, each consisting of t-ZrO_2.[14]

(3) Heating the $SP-ZrO_2$ to 500 °C in helium produces t-ZrO_2, and this phase persists upon cooling to room temperature in either an inert (He) or oxygen (or air) atmosphere.[14]

(4) Heating the $RP-ZrO_2$ to 500 °C in helium produces t-ZrO_2, and this phase persists if the sample is cooled to room temperature in an inert atmosphere. However, exposure of the $RP-ZrO_2$ sample that has been heated and then cooled to room temperature with air or oxygen results in the gradual transformation of t-ZrO_2 to m-ZrO_2. In addition, when the sample, following the 500 °C heating, is cooled in air, the $t \rightarrow m$ phase transition begins when the temperature reaches about 200 °C, and the transformation continues gradually with further cooling.[14]

(5) Both the $SP-ZrO_2$ and $RP-ZrO_2$ samples, dried in air at 110 °C, suffer a weight loss during heating in the temperature range from 100 to 400 °C, and mass spectrometry data show that water is evolved during the weight loss. The $RP-ZrO_2$ loses 0.8 H_2O/Zr and $SP-ZrO_2$ loses about 1 H_2O/Zr. Thus, if loss of water is a measure of the propensity of the material to the $t \rightarrow m$ transformation, $SP-ZrO_2$ would be expected to transform faster than $RP-ZrO_2$, and the data show the ease of transformation is contrary to this expectation.[22]

(6) Neither a weight loss nor evolution of water is observed for $RP-ZrO_2$ or $SP-ZrO_2$ during the exothermic event that produces t-ZrO_2. A poorly conducted experiment that contains too much sample in the TGA

(21) Clearfield, A. *J. Mater. Res.* **1991**, *5*, 161.
(22) Srinivasan, R.; Harris, M. B.; De Angelis, R. J.; Davis, B. H *J. Mater. Res.* **1988**, *3*, 787.

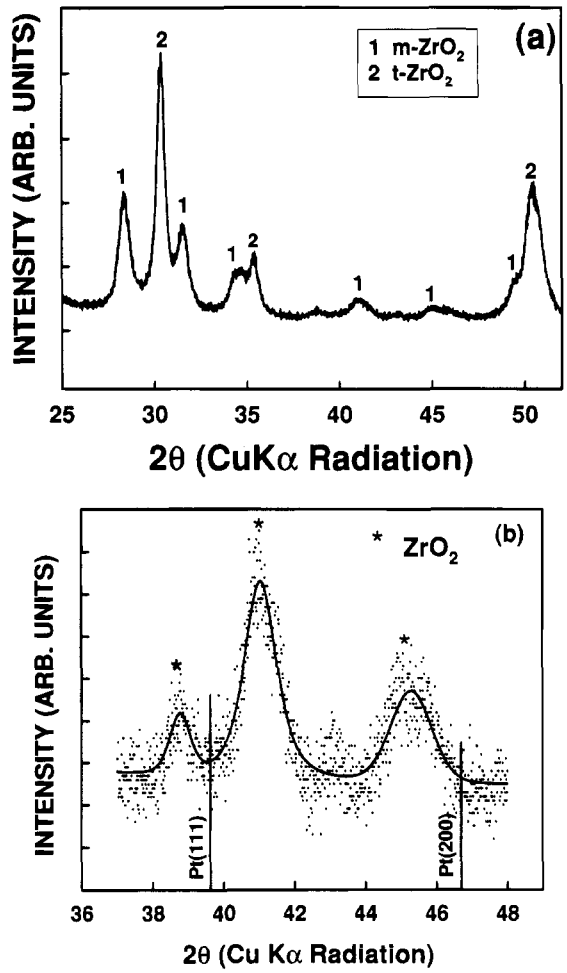

Figure 5. (a) X-ray diffraction pattern obtained from the Pt–SO_4^{2-}–ZrO_2 sample after being treated in H_2 in the TGA/DTA furnace. (b) Expanded XRD pattern in the 2θ region of 37–48°.

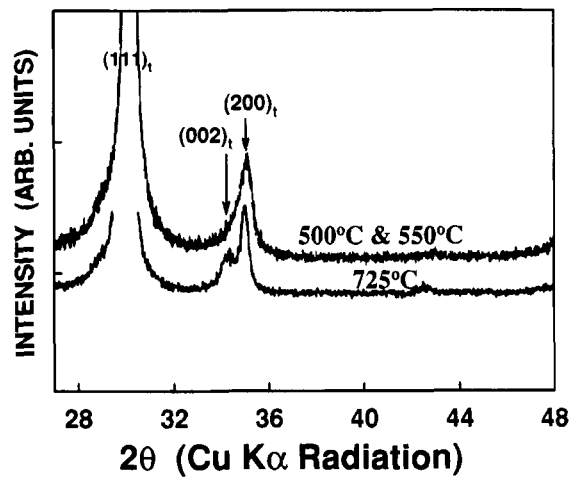

Figure 6. X-ray diffraction patterns obtained from the Pt–SO_4^{2-}–ZrO_2 sample following heating in H_2 at 500, 550, and 725 °C in the in situ X-ray diffractometer.

pan will result in a weight loss during the exothermic event; however, this is due to ZrO_2 being expelled from the pan, and this is indicated by the absence of MS data showing the loss of water or any other material with a mass of 1–100 amu, to account for the weight loss.[23]

(7) Either SP–ZrO_2 or RP–ZrO_2, following heating

(23) Srinivasan, R.; Davis, B. H., unpublished results.

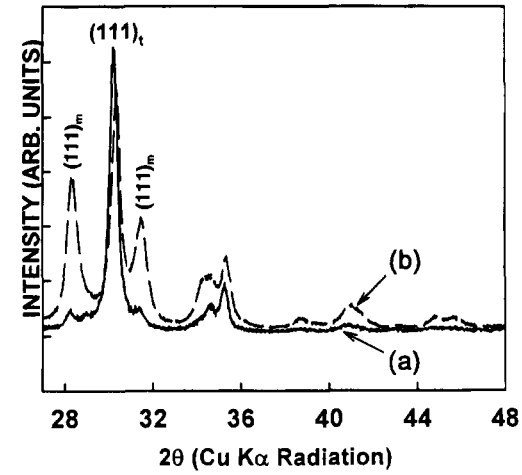

Figure 7. (a) X-ray diffraction pattern from the same sample as in Figure 6, after it was cooled to room temperature in H_2. (b) XRD pattern from this sample after exposure to air.

to 800 °C in an inert gas, exhibits a weight gain of about 0.6% upon subsequent cooling to room temperature in oxygen; unfortunately, the small weight gain precludes a valid determination of whether the amount of O_2 incorporated is the same, or different, for the two samples.[23] It was not possible to conduct simultaneously in situ weight gain measurements due to oxygen adsorption and XRD data showing the $t \rightarrow m$ transformation; however, the weight gain and $t \rightarrow m$ transformation show a similar trend during cooling in air.

(8) The weight loss vs temperature curves for SP– and RP–ZrO_2 samples have a similar shape. The surface area decreases from about 300 m^2/g to about 100 m^2/g during heating through the temperature region of the exothermic event.[24] Taking the area of OH^- to be the same as for N_2 (16.2 Å^2), one calculates that the weight loss for dehydroxylation by the reaction shown in eq 1 would be 1.8% for a 100 m^2/g surface that is fully hydroxylated. There is no evidence for this weight loss for either sample during heating above the exotherm at 450 °C. In other words, there is no weight loss data to indicate the occurrence of reaction 1 that corresponds to a fully hydroxylated surface.

The above eight statements, based upon experimental data, do not provide support for Clearfield's hypothesis as the reason for the ease of the $t \rightarrow m$ transformation, and most are at variance with the hypothesis. On the other hand, none of the above eight statements are at variance with the view that the transformation is triggered by oxygen adsorption.

It has been reported that oxygen adsorbs on zirconia as the temperature is lowered and triggers the tetragonal to monoclinic transformation.[13] The presence of sulfate is viewed to stabilize the tetragonal phase by covering the sites that adsorb oxygen and trigger the transformation.[20] Thus, following calcination in air, sufficient SO_4^{2-} is believed to remain on the surface so as to retard the phase transformation; this is not believed to be the case when the sample is treated in hydrogen. In contrast, following hydrogen treatment at 725 °C, the surface sulfur content is not sufficient to inhibit the adsorption of oxygen upon exposure to air, and the subsequent phase transformation that is trig-

(24) Srinivasan, R.; Davis, B. H. *J. Colloid Interface Sci.* **1993**, *156*, 400.

gered by oxygen adsorption. The presence of platinum does not appear to inhibit oxygen adsorption on zirconia surface to effect the phase transformation.

Metallic platinum is observed following calcination in air at 725 °C. However, following treatment in hydrogen at 725 °C or lower temperatures, metallic platinum is not observed by XRD. Presumably this is due to the reduction of platinum to the metallic state at the lower temperatures to produce either atomically dispersed platinum or metal crystallites that are too small to be detected by the XRD technique.

Conclusions

The current data indicate that when sulfate ions are present on the surface of zirconia, the platinum species is converted to its metallic state in air. Platinum particles in the range 4–6 nm were observed after activation in air at 725 °C for 2 h. However, metallic platinum was not observed after treatment in hydrogen at 725 °C. It appears that platinum is present in a highly dispersed state following treatment in H_2 environment. The oxygen-deficient surface sites on the zirconia appear to initiate the $t \rightarrow m$ phase transformation of the zirconia support, but this transformation is retarded when SO_4^{2-} is present.

Acknowledgment. The high-resolution electron microscopy work was carried out at the Center for High Resolution Electron Microscopy, Center for Solid State Sciences, Arizona State University. Valuable assistance by Dr. M. McCartney and Prof. D. J. Smith is acknowledged. This research was sponsored by the Commonwealth of Kentucky and by the U.S. Department of Energy, Assistant Secretary for Energy Efficiency and Renewable Energy, Office of Transportation Technologies, as part of the High Temperature Materials Laboratory User Program under Contract DE-AC05-844OR21400, managed by Martin Marietta Energy Systems, Inc. The research was supported in part by an appointment to the Oak Ridge National Laboratory Postdoctoral Research Associates Program administered jointly by the Oak Ridge National Laboratory and Oak Ridge Institute for Science and Education.

CM940504U